Searches for strong production of supersymmetric particles

THE UNIVERSITY of ADELAIDE

Edmund Ting

o.b.o. the ATLAS Collaboration

SUSY24, IFT Madrid

ATLAS EXPERIMENT

introduction

- supersymmetry (SUSY) is an extension to the Standard Model that presents solutions for e.g. dark matter, hierarchy problem
- prime target of study at colliders due to rich particle content
- useful in the context of collider searches: provides framework that encompasses many experimentally observable signatures
  - final state of various "regular" particles (electrons, jets, etc.)
  - more exotic: displaced objects [Vasiliki's and Alexander's talks]
- strong production of SUSY particles (squarks and gluinos) interesting due to higher theoretical cross-sections
  - summary of recent EW results in Alessandro's and Jeff's talks

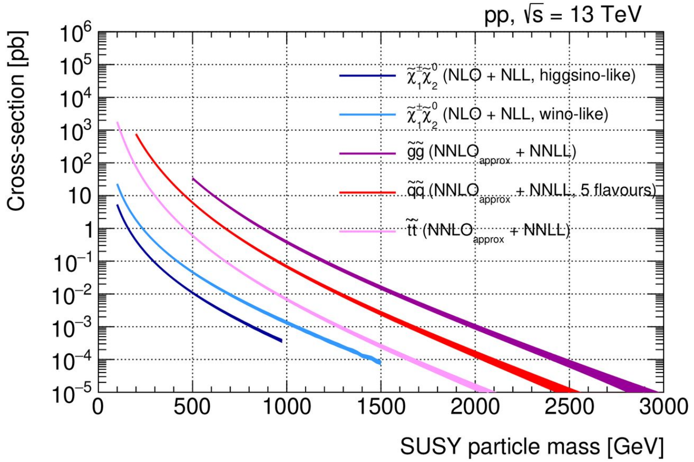

overview

- [many results already published by ATLAS] (and other experiments) targeting various regions of parameter space
- today's talk will focus on two recent ATLAS results motivated by RPC SUSY using 140 fb^{-1} of Run 2 data:
  - Search for new phenomena with top-quark pairs and large missing transverse momentum [tt+MET] *JHEP 03 (2024) 139*
  - Search for top-squark pair production in final states containing a top quark, a charm quark and missing transverse momentum [tc+MET] *arXiv:2402.12137*
- RPV SUSY results: see [Yvonne's talk]

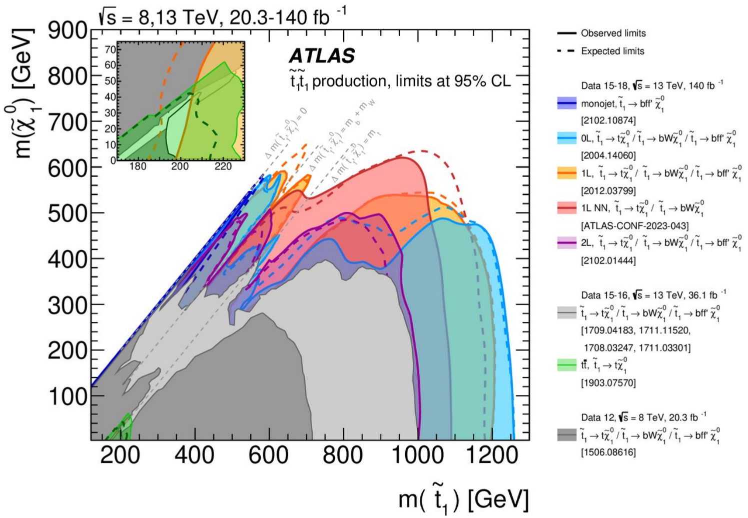

stop to top — signal model

- searching for events with final state containing one **hadronically-decaying top**, one **leptonically-decaying top**, and large **missing transverse momentum**
- signature motivated by several scenarios:
  - SUSY: direct $\tilde{t}_1$ pair production with two- or three-body decays to $t+\tilde{\chi}_1$
  - DM fermions via (pseudo) scalar mediator in association with top quarks
  - *ttνν* from effective four-fermion contact interaction (SMEFT)
- uses the full 140 fb^{-1} Run 2 dataset
  - improves on previous ATLAS $\tilde{t}_1\tilde{t}_1$ result by using better object reconstruction and identification, background simulation, and neural networks for signal classification
  - results statistically combined with the all-hadronic stop search

JHEP 04 (2021) 174

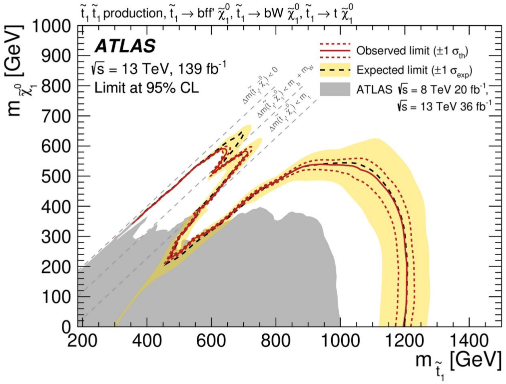

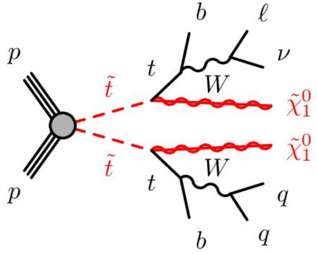

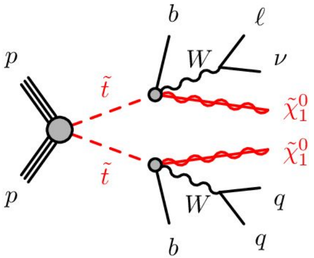

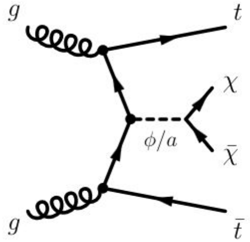

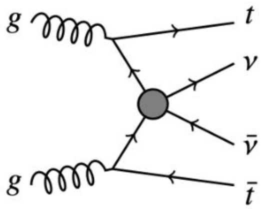

stop to top — analysis strategy

Signature-based search strategy: partition events based on object multiplicities.

Novel approach that provides sensitivity to a **wide range of parameter space**.

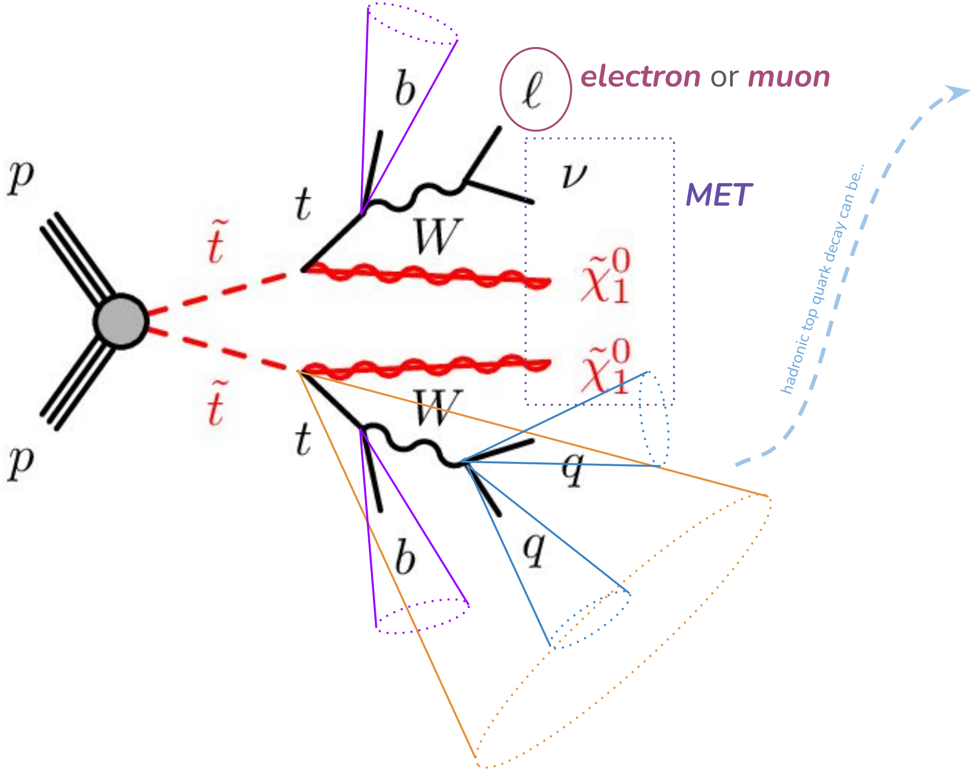

Resolved (p_T < 600 GeV): "top-NN"

- assigns score to all two and three (small-R) jet combinations (with exactly 1 b-jet) in event
- combination with highest NN output value in each event is chosen as the top candidate
- 70% selection efficiency for top quarks with 200 GeV < p_T < 600 GeV

Boosted (p_T > 600 GeV):

- reconstructed as large-R jet
- multivariate classifier uses substructure to tag top jets with 80% efficiency

stop to top — analysis strategy

All signal regions are required to have 1 e/μ and no $\tau_{had.}$ candidates.

Split into two categories depending on the large-R jet multiplicity:

$N_{large\text{-}R} = 0$

"High-MET"

further split into '1b' and '2b' for events containing exactly one, or two or more, b-tagged jets

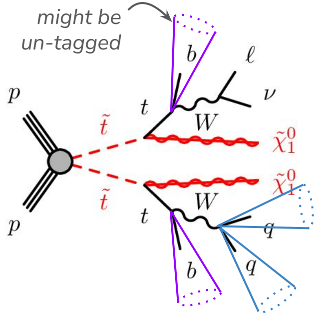

$N_{large\text{-}R} \geq 1$

"Boosted"

six orthogonal regions depending on whether large-R jet is top-tagged, and the number of b-tagged jets (1 or 2+) and whether they lie inside or outside the large-R jet

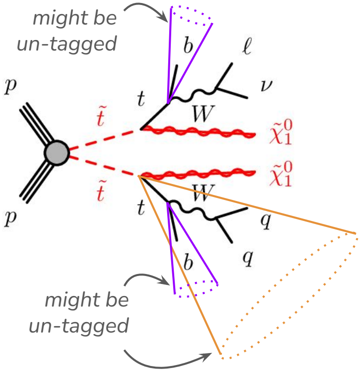

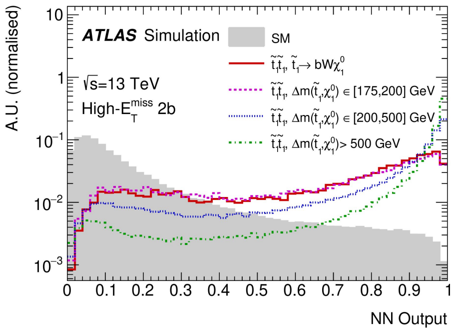

stop-NN
high-MET '2b'

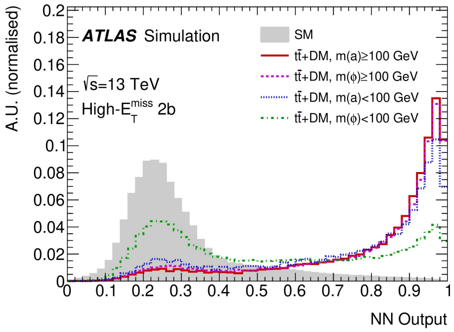

DM-NN
high-MET '2b'

For each region defined, a NN classifier is trained, using SUSY signal events from **across parameter space**.

In high-MET regions, a second NN is also trained with tt+DM events as the signal.

stop to top — backgrounds

main backgrounds: **$t\bar{t}Z$**, **$t\bar{t}$1L**, **$t\bar{t}$2L**, ***W*** and **single-top**

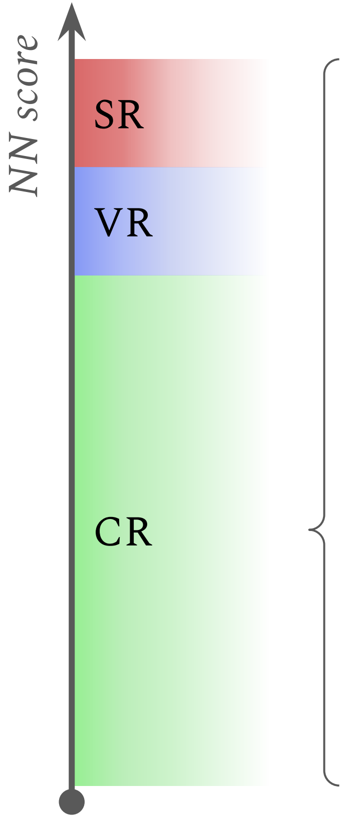

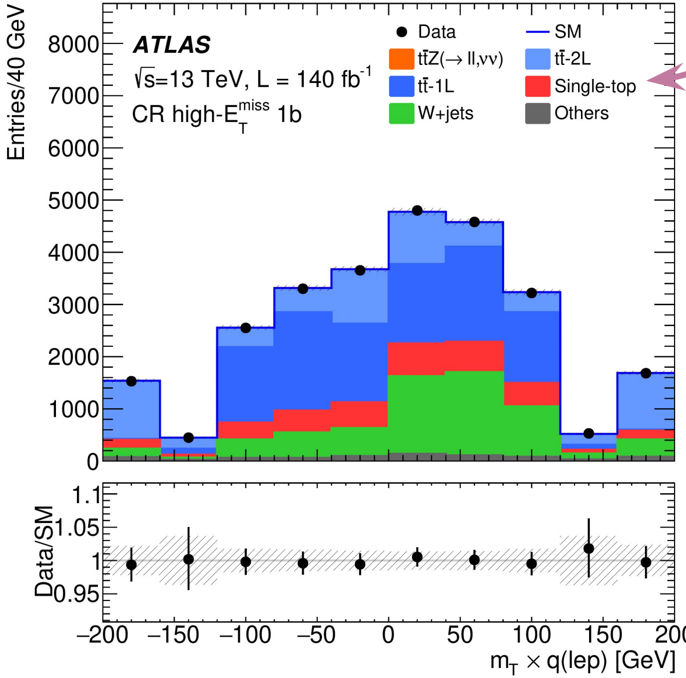

CRs binned in m_T * q(ℓ). Backgrounds with 1 leptonically-decaying *W* have endpoint at m_W (i.e. all but *tt*2L). Lepton charge discriminates between *W*+jets and *tt*1L (different xsec for W^+ and W^-).

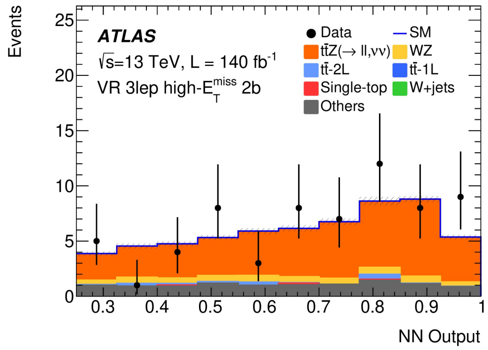

ttZ(→νν) has low cross section but identical signature as signal. Not fitted; validated in 3 lepton VRs with two SFOS leptons compatible with *Z* (mimic ν in SRs by vectorially adding to MET)

Normalisation factors derived for *tt*1L, *tt*2L, *W* and single-top backgrounds.

stop to top — results

- good agreement between data and MC in all CRs, VRs and SRs
  - NFs for fitted backgrounds compatible with unity;
    largest u/c for single top, related to *tW* diagram removal
  - in SRs, largest deviations (~2σ) seen in regions with 2 *b*-tagged jets
- **no significant excess** ➡ set limits (combined with previous analyses)
  - SUSY: exclusion limits using CL_S @ 95% CL
  - DM: upper limits on production cross-section

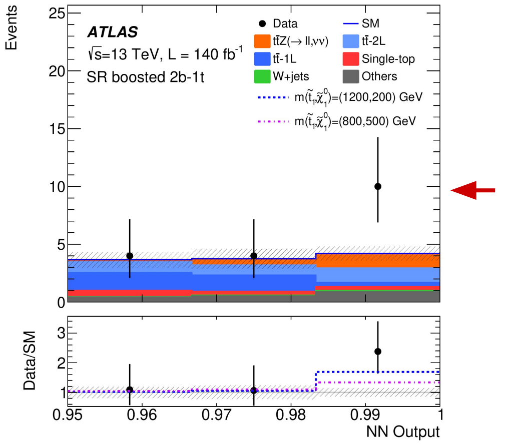

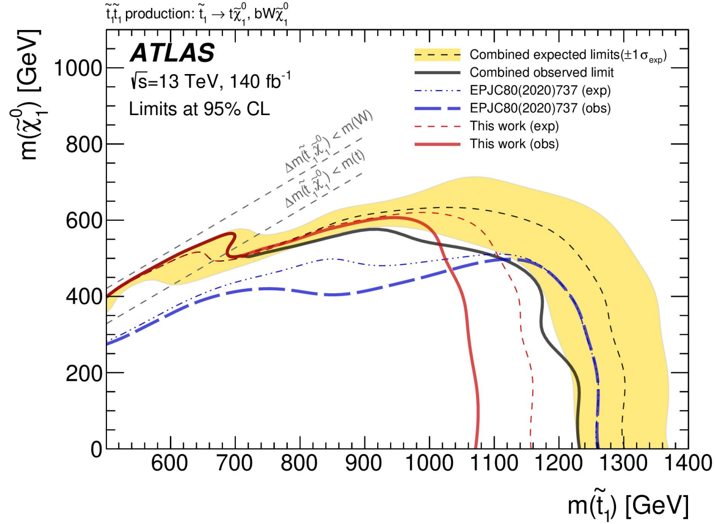

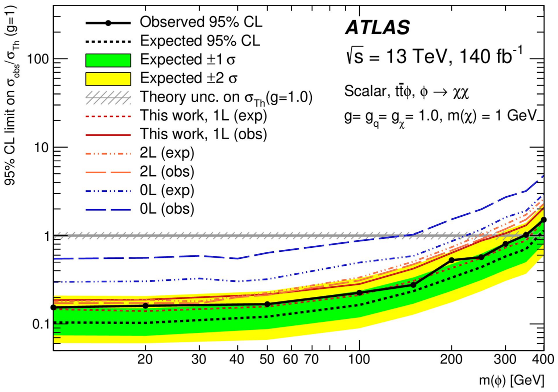

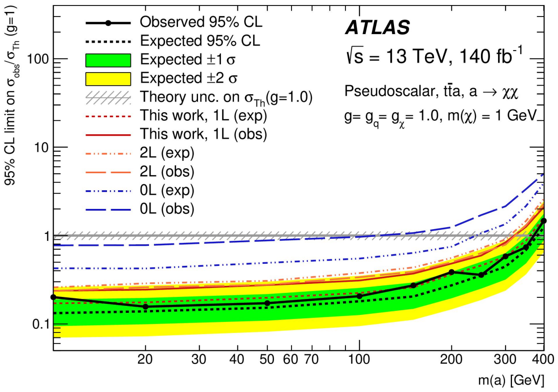

dominant sources of uncertainty: data statistics, background theory

stop to top or charm — signal model

first LHC result in this final state!

- stop pair production with decay to neutralino and SM top or charm
- motivated by non-minimal flavour violating extensions of MSSM
- only consider scenarios where top can be produced on-shell: $\Delta m(\tilde{t}_1, \tilde{\chi}_1) \geq 175$ GeV
- final state: **hadronically-decaying top**, **charm quark**, and large **missing transverse momentum**

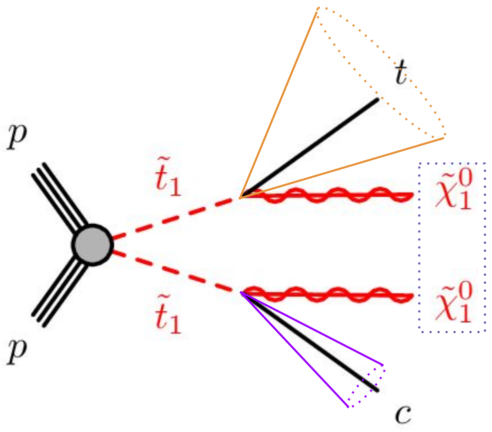

b-tagging is well-established… *c*-tagging not so much!

- high-level DNN tagger (DL1r) leverages jet topology, impact parameter taggers, and secondary vertex finding algorithms
- multidimensional output (p_b, p_c, p_{light}) combined for *c*-tagging
- *b*-tag takes precedence: avoids high *b*-mistag rates

$$\mathrm{DL1r}_c = \log\left(\frac{p_c}{f_b p_b + (1 - f_b) p_u}\right)$$

ε_c	*b*-rej.	light rej.
20%	29	57

stop to top or charm — analysis strategy

Four **signal regions** targeting **different regions of parameter space**.

Trigger on **missing transverse momentum** (MET);
require zero **leptons** (e/μ), ≥1 ***b*-tagged** and ≥1 **c-tagged** jet.
Orthogonal by choice of additional selections.

SRA (*bulk*):

- high m_{T2} (stransverse mass between top- and *c*-tagged jets)

SRB, SRC (*intermediate*):

- binned in $m_T(j,MET)_{close}$ for increased sensitivity

SRD (*compressed*):

- strong **ISR** topology to facilitate high MET
- multi-class neural network to separate **signal** from ***tt***-like and ***V*+jets**-like events
- binned in m_{eff} and $m_T(j,MET)_{close}$

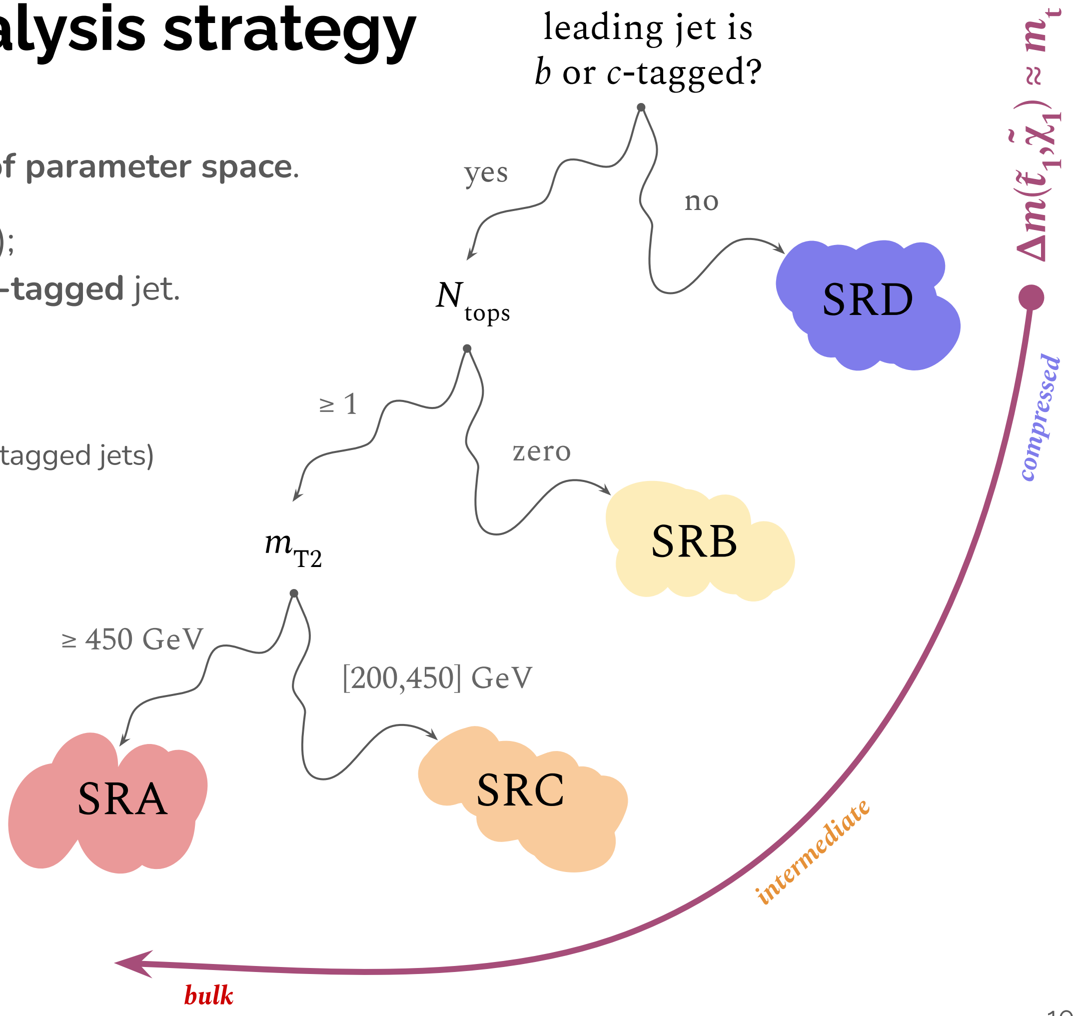

stop to top or charm — backgrounds

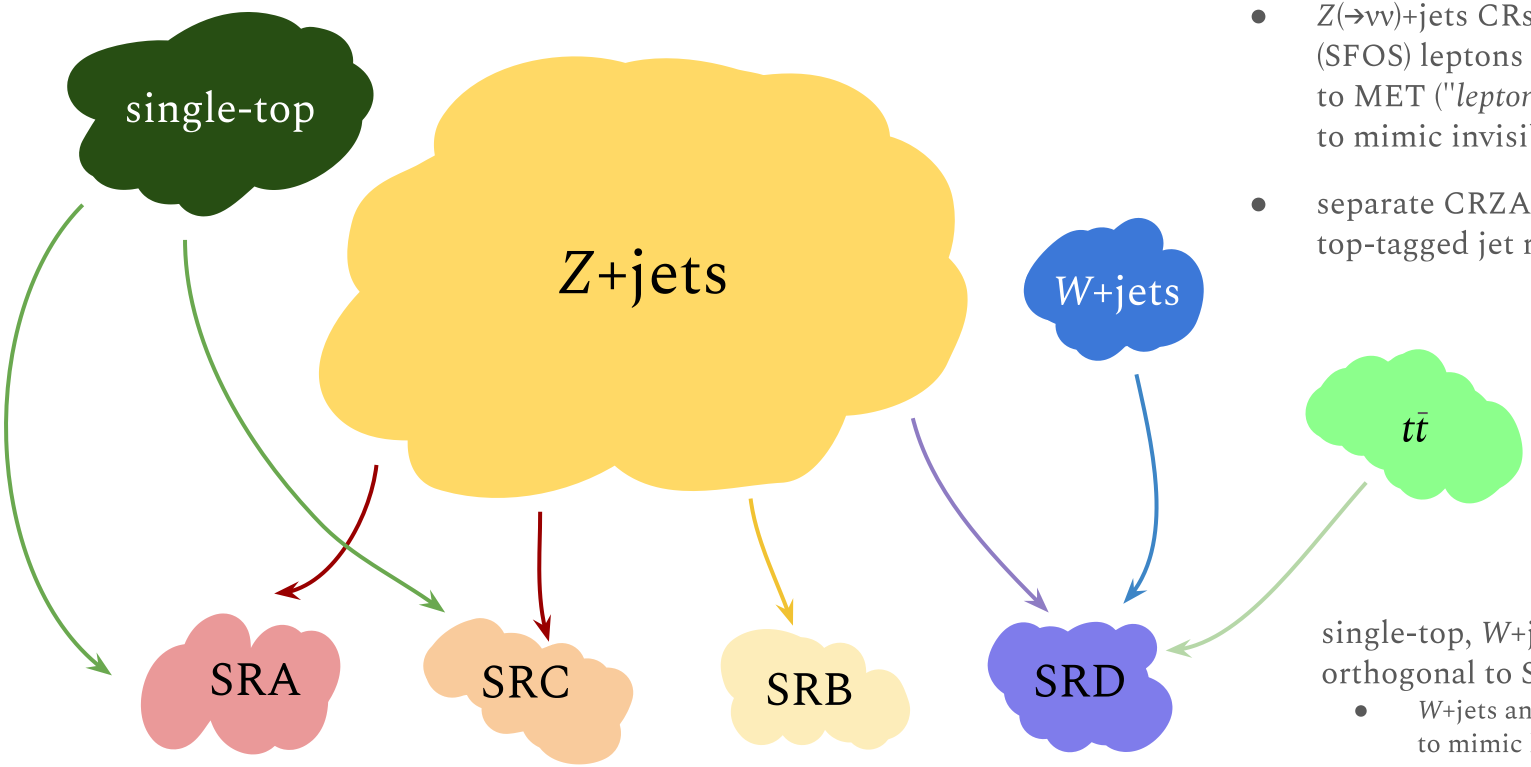

- $Z(\rightarrow\nu\nu)$+jets CRs defined with 2 (SFOS) leptons required. Added to MET ("*lepton-corrected MET*") to mimic invisible *Z*-decay in SR
- separate CRZAC and CRZB with top-tagged jet requirement/veto

single-top, *W*+jets and *tt* CRs are orthogonal to SRs via 1ℓ selection

- *W*+jets and *tt*: treat lepton as jet to mimic hadronically-decaying τ in SR

a **control region** (CR) *is defined for each set of different-coloured arrows to estimate that background in the SRs indicated*

stop to top or charm — results

- multi-bin fits: background-only (CR-only), model-dependent (CR+SR); incl.: model-independent

- fitted backgrounds:
  - A/B/C: *Z*+jets, single-top
  - D: *Z*+jets, *W*+jets, three NFs for $t\bar{t}$ (one per m_{eff} bin)

- dominant uncertainties:
  - A: experimental uncertainties related to large-*R* jets
  - B/C: selections on the *b*- and *c*-jet p_T
  - D: *W*+jets normalisation uncertainty

- **no significant excesses** found in observed data
  - largest deviation of 2σ in SRs with tightest m_{T2} cuts

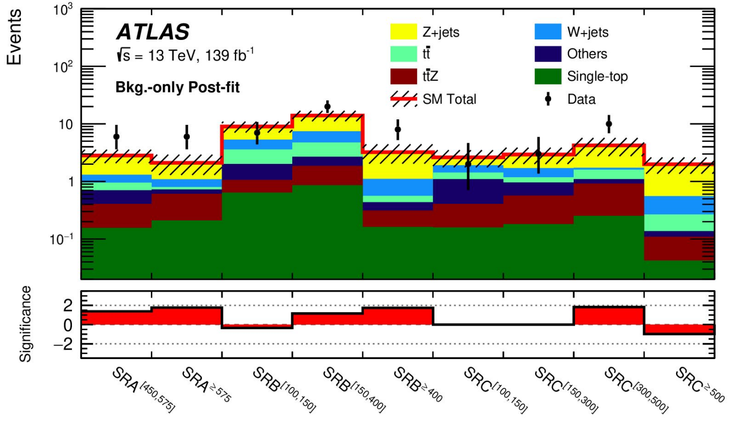

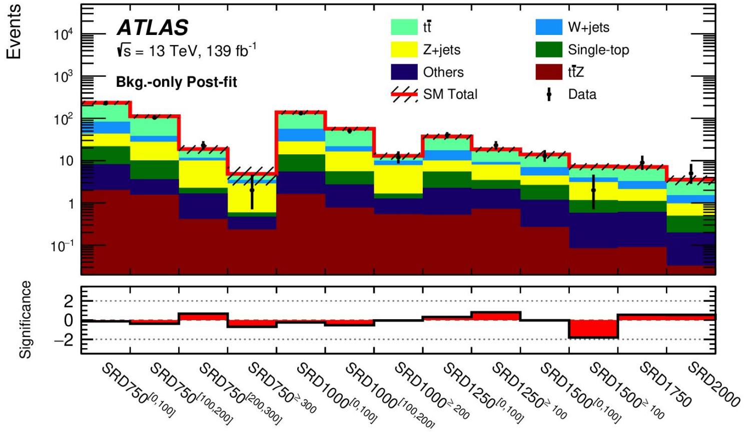

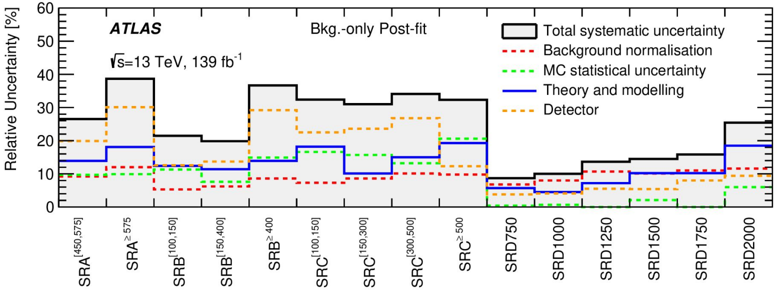

stop to top or charm — results

- exclusion limits placed in the $m(\tilde{t}_1)$–$m(\tilde{\chi}_1)$ plane
  - $BR(\tilde{t}_1 \to t\tilde{\chi}_1) = 50\%$
  - scan over BR for $m(\tilde{\chi}_1)$ = 1 GeV
- model-independent interpretation: upper limits for visible cross-section and number of signal events at 95% CL (*see backup*)

$m(\tilde{t}_1) \lesssim$ 800 GeV excluded for high mass,
$m(\tilde{t}_1) \lesssim$ 600 GeV for compressed

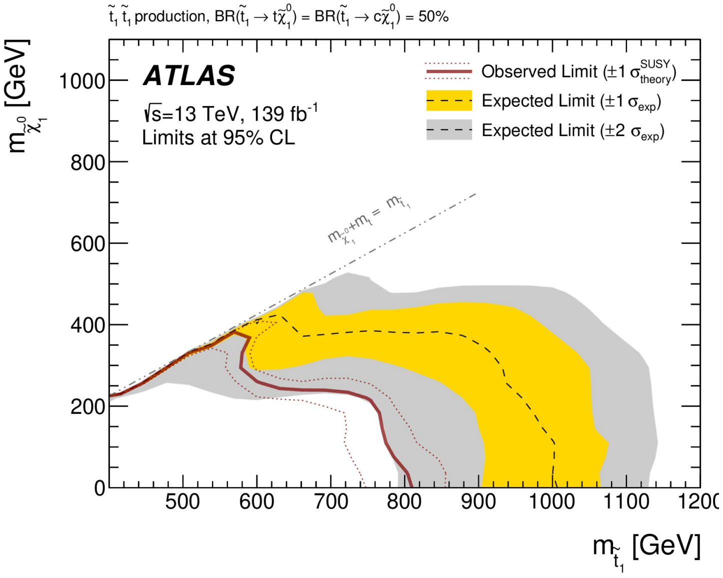

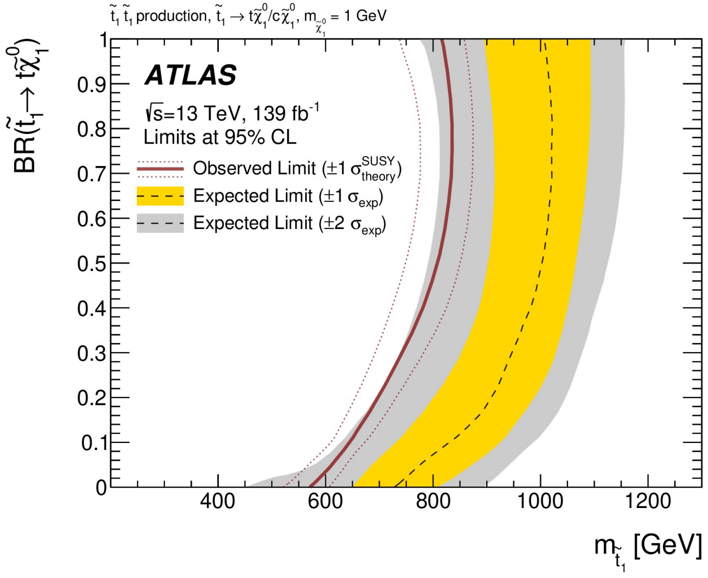

summary and outlook

- two new results using Run 2 data presented in this talk
  - strong production of stops motivated by RPC SUSY
  - novel ML-based analysis strategies featuring improved background modelling, object reconstruction, …
- no significant excesses seen over SM backgrounds
  - limits set on stop pair production cross-section
  - including interpretations in DM models
- Run 3 ongoing: many new analyses in the works!
- looking to the future: high-luminosity upgrade will grant ~10x more integrated luminosity @ 14 TeV
  - recent pub-note exploring prospects of tt+MET (2ℓ) at HL-LHC given the expected luminosity scaling

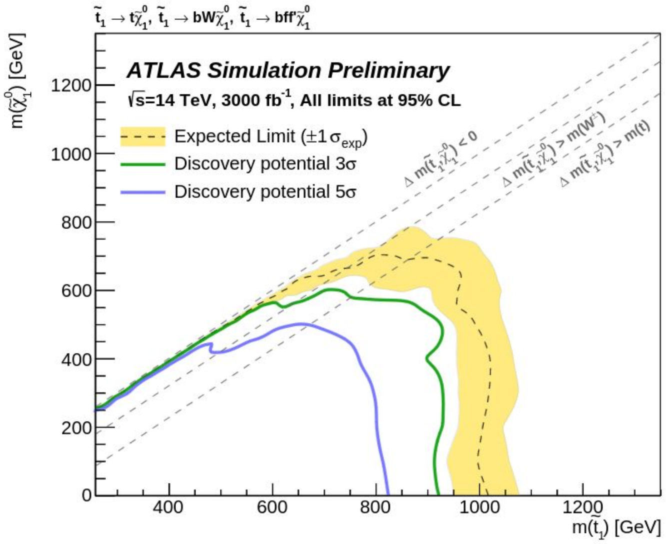

backup

backup — tt+MET SR definitions

Analysis Category	High-E_T^{miss} 1b	High-E_T^{miss} 2b	Boosted 1b-lep-0t	Boosted 1b-had-0t	Boosted 2b-0t	Boosted 1b-lep-1t	Boosted 1b-had-1t	Boosted 2b-1t
$N(lR\text{ jet}, p_T > 600\text{ GeV})$	0		≥ 1					
$N(\text{top-tagged } lR\text{ jet})$	-		0			≥ 1		
$N_{b-\text{jet}}$ with $\Delta R(b, lR\text{ jet}) < 1.1$	-		0	≥ 1	≥ 1	0	≥ 1	≥ 1
$N_{b-\text{jet}}$ with $\Delta R(b, lR\text{ jet}) > 1.1$	-		≥ 1	0	≥ 1	≥ 1	0	≥ 1
top-NN-tagged multiplet	✓		-					
$N_{b-\text{jet}}$	1	≥ 2	-					
$N_{\text{light-jet}}$	≥ 2	≥ 1	-					
top_{had} candidate	top-NN multiplet		lR jet					
top_{lep} candidate	$\ell + j$	$\ell + b$	$\ell + b$	$\ell(+j)$	$\ell + b$	$\ell + b$	$\ell(+j)$	$\ell + b$

Category	stop-NN CR Range	stop-NN VR Range	stop-NN SR Range	stop-NN Eff.	DM-NN CR Range	DM-NN VR Range	DM-NN SR Range	DM-NN Eff.
High-E_T^{miss} 1b	[0.2, 0.64)	[0.64, 0.79)	[0.79, 1.0]	0.4-0.9	[0.3, 0.69)	[0.69, 0.87)	[0.87, 1.0]	0.3-0.4
High-E_T^{miss} 2b	[0.1, 0.56)	[0.56, 0.70)	[0.70, 1.0]	0.5-0.9	[0.3, 0.60)	[0.60, 0.76)	[0.76, 1.0]	0.6-0.8
Boosted 1b-lep-1t	[0.0, 0.65)	[0.65, 0.80)	[0.80, 1.0]	0.5-0.9				
Boosted 1b-had-1t	[0.0, 0.65)	[0.65, 0.85)	[0.85, 1.0]	0.6-0.9				
Boosted 2b-1t	[0.0, 0.75)	[0.75, 0.95)	[0.95, 1.0]	0.6-0.8				
Boosted 1b-lep-0t	[0.0, 0.70)	[0.70, 0.85)	[0.85, 1.0]	0.6-0.8				
Boosted 1b-had-0t	[0.0, 0.75)	[0.75, 0.95)	[0.95, 1.0]	0.4-0.8				
Boosted 2b-0t	[0.0, 0.65)	[0.65, 0.80)	[0.80, 1.0]	0.6-0.9				

backup — tt+MET

normalisation factors (*high-MET regions*)

NF(*tt*1L)	NF(*tt*2L)	NF(*W*+jets)	NF(s.t.)
1.02 ± 0.06	1.09 ± 0.05	1.30 ± 0.15	1.4 ± 0.4

dominant uncertainties

	$\tilde{t}_1\tilde{t}_1$, $m(\tilde{t}_1,\tilde{\chi}^0_1)$ GeV		$t\bar{t}$+DM, $m(a,\chi)$ GeV	
	(1000, 600)	(1200, 200)	(50, 1)	(150, 1)
$\mu \pm \sigma(\mu)$ (total uncertainty)	$0.25^{+0.42}_{-0.25}$	$0.8^{+0.7}_{-0.5}$	$0.08^{+0.10}_{-0.08}$	$0.12^{+0.13}_{-0.12}$
Data statistical uncertainty	82 %	74 %	67 %	69 %
Background modelling	45 %	62 %	51 %	48 %
MC statistical uncertainty	25 %	20 %	34 %	33 %
Jet energy scale and resolution	20 %	13 %	29 %	28 %
Flavour tagging efficiency	18 %	10 %	21 %	21 %

constraints on effective *ttvv* contact interactions

Table 6: Constraints on effective $t\bar{t}\nu\bar{\nu}$ contact interactions involving all three generations of left-handed neutrinos based on the results of the $\tilde{t}_1\tilde{t}_1$ search. Constraints are set independently for different effective vector operators and for different hypotheses about the sign of the Wilson coefficient which leads to a constructive or destructive interference with $t\bar{t}Z(\rightarrow \nu\bar{\nu})$. Observed (expected) limits at 95% CL are reported for $\sqrt{|V_{ij}|}/\Lambda$ and for Λ, for the full phase space and for specified regions of the true invariant mass of the neutrino pair, assuming $|V_{ij}| = 4\pi$. Limits corresponding to $\pm 1\sigma$ variations of the expected limits are also reported.

Wilson coefficient	Observed (Expected) upper limit on $\sqrt{\lvert V_{ij}\rvert}/\Lambda$ [TeV^{-1}]	Observed (Expected) lower limit on Λ for $\lvert V_{ij}\rvert = 4\pi$ [TeV]
$V_{LL} > 0$	$1.59\ (1.44^{1.58}_{1.31})$	$2.23\ (2.47^{2.71}_{2.25})$
$m_{\nu\bar{\nu}} < 1$ TeV	$1.84\ (1.66^{1.82}_{1.51})$	$1.93\ (2.14^{2.35}_{1.95})$
$m_{\nu\bar{\nu}} < 2$ TeV	$1.62\ (1.46^{1.61}_{1.36})$	$2.18\ (2.42^{2.66}_{2.21})$
$V_{LL} < 0$	$1.66\ (1.52^{1.66}_{1.40})$	$2.13\ (2.33^{2.53}_{2.14})$
$m_{\nu\bar{\nu}} < 1$ TeV	$1.96\ (1.80^{1.95}_{1.66})$	$1.81\ (1.97^{2.13}_{1.82})$
$m_{\nu\bar{\nu}} < 2$ TeV	$1.70\ (1.56^{1.69}_{1.44})$	$2.08\ (2.28^{2.47}_{2.10})$
$V_{LR} > 0$	$1.67\ (1.53^{1.66}_{1.40})$	$2.12\ (2.32^{2.53}_{2.13})$
$m_{\nu\bar{\nu}} < 1$ TeV	$1.92\ (1.78^{1.94}_{1.64})$	$1.84\ (1.99^{2.16}_{1.82})$
$m_{\nu\bar{\nu}} < 2$ TeV	$1.70\ (1.56^{1.70}_{1.44})$	$2.08\ (2.27^{2.47}_{2.08})$
$V_{LR} < 0$	$1.63\ (1.49^{1.63}_{1.36})$	$2.17\ (2.38^{2.60}_{2.18})$
$m_{\nu\bar{\nu}} < 1$ TeV	$1.86\ (1.72^{1.89}_{1.58})$	$1.91\ (2.06^{2.25}_{1.88})$
$m_{\nu\bar{\nu}} < 2$ TeV	$1.66\ (1.52^{1.67}_{1.40})$	$2.13\ (2.33^{2.54}_{2.13})$

backup — tt+MET comparison to previous analysis

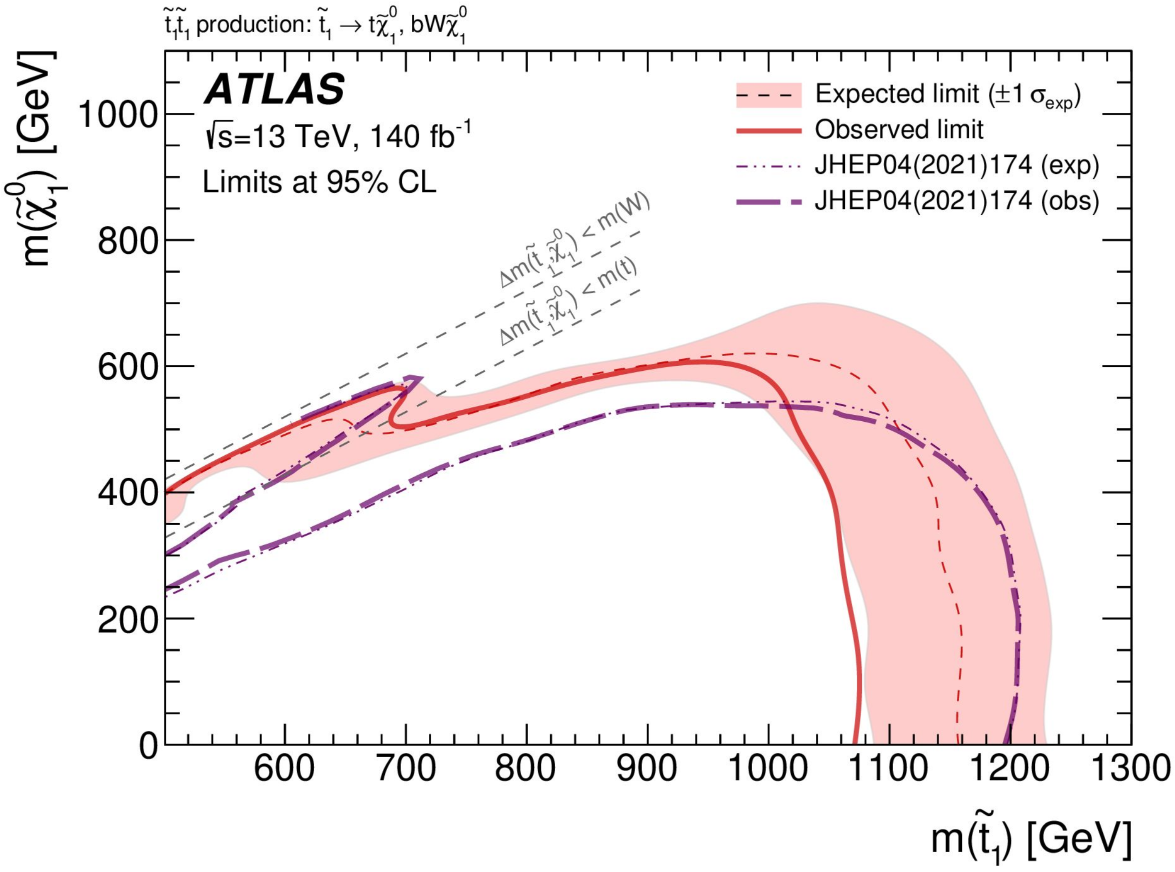

backup — tc+MET postfit agreement in CRs and VRs

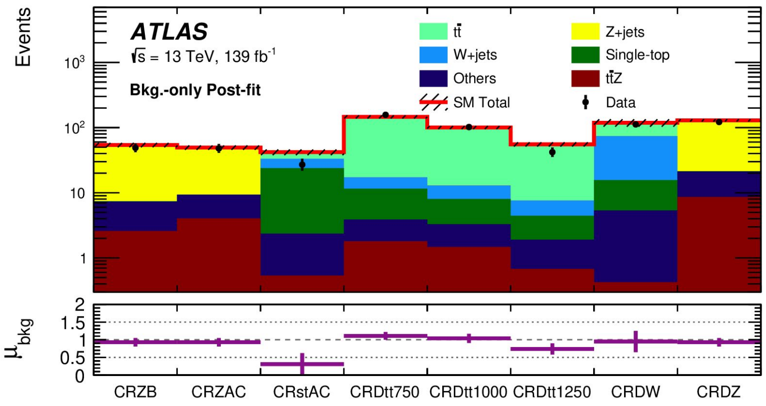

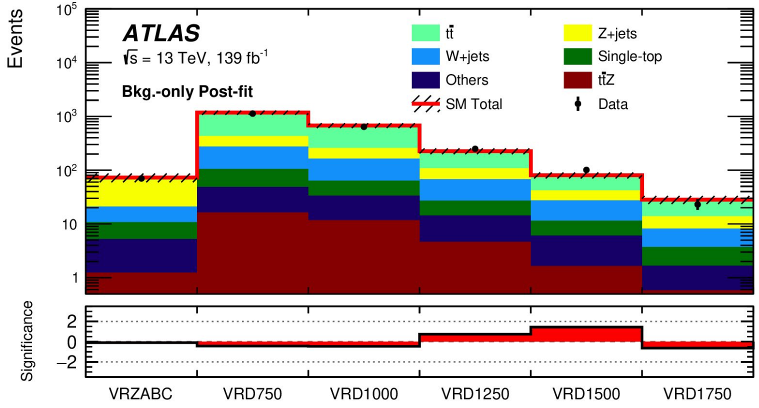

Large discrepancy and uncertainty in CRstAC driven by comparisons of DR vs DS schemes.

backup — tc+MET model-independent limits

Signal region	$\langle\epsilon\sigma\rangle^{95}_{\mathrm{obs}}$[fb]	S^{95}_{obs}	S^{95}_{exp}	CL_{B}	p_0 (Z)
SRA ($m_{\mathrm{T2}}(j^b_{R=1.0}, c) \geq 450$ GeV)	0.10	14.4	$8.4^{+3.5}_{-1.9}$	0.94	0.02 (2.1)
SRA ($m_{\mathrm{T2}}(j^b_{R=1.0}, c) \geq 575$ GeV)	0.07	9.4	$5.8^{+2.9}_{-1.2}$	0.89	0.04 (1.7)
SRB ($m_{\mathrm{T}}(j, E^{\mathrm{miss}}_{\mathrm{T}})_{\mathrm{close}} \geq 100$ GeV)	0.17	24.1	$16.8^{+7.0}_{-5.2}$	0.85	0.09 (1.3)
SRB ($m_{\mathrm{T}}(j, E^{\mathrm{miss}}_{\mathrm{T}})_{\mathrm{close}} \geq 150$ GeV)	0.16	22.8	$13.2^{+5.5}_{-3.6}$	0.95	0.03 (1.9)
SRB ($m_{\mathrm{T}}(j, E^{\mathrm{miss}}_{\mathrm{T}})_{\mathrm{close}} \geq 400$ GeV)	0.08	11.3	$6.5^{+3.1}_{-1.6}$	0.92	0.04 (1.8)
SRC ($m_{\mathrm{T}}(j, E^{\mathrm{miss}}_{\mathrm{T}})_{\mathrm{close}} \geq 100$ GeV)	0.09	12.6	$9.6^{+4.2}_{-2.1}$	0.76	0.22 (0.76)
SRC ($m_{\mathrm{T}}(j, E^{\mathrm{miss}}_{\mathrm{T}})_{\mathrm{close}} \geq 150$ GeV)	0.09	11.9	$8.7^{+3.9}_{-1.9}$	0.81	0.15 (1.0)
SRC ($m_{\mathrm{T}}(j, E^{\mathrm{miss}}_{\mathrm{T}})_{\mathrm{close}} \geq 300$ GeV)	0.08	11.0	$7.8^{+3.6}_{-1.7}$	0.83	0.13 (1.1)
SRC ($m_{\mathrm{T}}(j, E^{\mathrm{miss}}_{\mathrm{T}})_{\mathrm{close}} \geq 500$ GeV)	0.02	2.5	$4.0^{+2.4}_{-1.4}$	0.13	0.50 (0.00)
SRD ($m_{\mathrm{eff}} \geq 750$ GeV, $m_{\mathrm{T}}(j, E^{\mathrm{miss}}_{\mathrm{T}})_{\mathrm{close}} \geq 200$ GeV)	0.15	20.4	$18.5^{+8.4}_{-5.1}$	0.58	0.50 (0.00)
SRD ($m_{\mathrm{eff}} \geq 1000$ GeV, $m_{\mathrm{T}}(j, E^{\mathrm{miss}}_{\mathrm{T}})_{\mathrm{close}} \geq 200$ GeV)	0.10	13.9	$13.7^{+3.5}_{-5.7}$	0.52	0.50 (0.00)
SRD ($m_{\mathrm{eff}} \geq 1250$ GeV)	0.30	41	37^{+12}_{-11}	0.60	0.50 (0.00)
SRD ($m_{\mathrm{eff}} \geq 1500$ GeV)	0.09	12.9	$14.6^{+6.3}_{-4.1}$	0.36	0.50 (0.00)
SRD ($m_{\mathrm{eff}} \geq 1750$ GeV)	0.09	12.1	$9.1^{+3.9}_{-1.9}$	0.77	0.20 (0.84)
SRD ($m_{\mathrm{eff}} \geq 2000$ GeV)	0.05	7.3	$5.6^{+3.0}_{-1.2}$	0.70	0.26 (0.64)